Cumulus Entrainment and Cloud Droplet Spectra: A Numerical Model within a Two-Dimensional Dynamical Framework

JEAN-LOUIS BRENGUIER

METEO-FRANCE, CNRM, France

WOJCIECH W. GRABOWSKI*

National Center for Atmospheric Research,† Boulder, Colorado

(Manuscript received 12 September 1991, in final form 13 April 1992)

ABSTRACT

A simple numerical model designed to predict the evolution of cloud droplet spectra with special emphasis on the role of entrainment is developed for a case of nonprecipitating cloud. The model assumes that the cloud water mixing ratio at any grid location is equal to that predicted by a cloud model using bulk microphysics; that is, supersaturation/undersaturation inside cloud is neglected. Locally, only undiluted droplet concentrations are assumed to exist; any average dilution of cloud droplet concentration observed over a grid volume is interpreted as an effect of internal structure within the grid, with undiluted cloudy patches coexisting with those that are cloud free. Activation of cloud condensation nuclei is assumed to always produce the same initial spectrum of cloud droplets. Further condensational growth of this initial spectrum produces a set of base functions that are used to represent droplet spectral evolution.

The microphysical model, combined with the two-dimensional cloud model using bulk microphysics, is applied to an idealized case of small cumulus. It is shown that, within the current framework, entrainment usually leads to fresh activation of cloud droplets and results in multimodal spectra in actively growing cells. Both broad and narrow cloud droplet spectra are predicted in old, highly diluted cells at cloud periphery. These results are discussed in the context of both observational and theoretical studies of droplet spectral evolution.

1. Introduction

Understanding the influence of entrainment on cloud droplet spectra is a challenging problem. This is mainly because of the large span of spatial scales that are involved in this process. The large-scale end of this spectrum, at which an "entrainment event" is initiated, is associated with scales not much smaller than the cloud itself. As the mixing progresses, smaller- and smaller-scale motions result as kinetic energy is transferred toward small scales and finally dissipated when the Kolmogorov microscale is reached. As pointed out by Jensen and Baker (1989), the spectrum of *existing* cloud droplets is mainly influenced when the Kolmogorov microscale is approached. At the same time, fresh nucleation of cloud droplets in air parcels entrained into actively growing cloud may occur on a large spectrum of scales. Thus, allowance has to be made in cloud modeling for a synergic treatment of processes over a broad range of scales. In the traditional approach, model-predicted fields (as supersaturation or droplet concentration) are usually assumed to be homogeneous over the grid box.[1] Even with high spatial resolution (say, of the order of 1 m; Grabowski 1989), the grid size is still about three orders of magnitude coarser than the Kolmogorov microscale. Therefore, it is doubtful that the traditional approach is appropriate for studying the effects of entrainment and mixing on cloud droplet spectra.

In general, efficient and accurate modeling of physical process responsible for droplet spectral evolution is difficult. As far as condensation is concerned, nucleation and further condensational growth may be considered separately. Since number concentration and size distribution of nucleated droplets are the most important parameters determining further growth of droplet population, accurate modeling of the nucleation process is quite important. However, modeling

* On leave from Institute of Geophysics, Polish Academy of Science, Warsaw, Poland.

† The National Center for Atmospheric Research is sponsored by the National Science Foundation.

Corresponding author address: Dr. Wojciech W. Grabowski, P.O. Box 3000, National Center for Atmospheric Research, Boulder, CO 80307-3000.

[1] A subgrid-scale condensation scheme, for example, Sommeria and Deardorff 1977, formulated and used within a bulk cloud model, is an example of an approach in which this assumption is not made.

of the nucleation is computationally very demanding: many categories of cloud condensation nuclei (CCN) have to be introduced and small time steps must be used to ensure numerical stability. In the case of further growth of droplet population, a large enough number of droplet categories should be used, especially when not only mean diameter but also dispersion of the droplet distribution is of interest. In addition, prediction of the supersaturation field near steep gradients of thermodynamical variables (that is, near cloud edges) is numerically very difficult in high-resolution calculations (Grabowski 1989; Grabowski and Smolarkiewicz 1990).

This paper presents a different approach. The main assumption is that cloud droplet concentration on the subgrid scale always corresponds to that resulting from nucleation. When the droplet concentration observed on the model grid is less than the undiluted one, it is assumed that the grid volume consists of a cloudy part, with an undiluted droplet concentration, and a cloud-free part. This situation corresponds to the extremely inhomogeneous mixing (Baker et al. 1980). Nucleation of cloud droplets is not calculated explicitly, but it is assumed to produce a prescribed spectrum of cloud droplets. Droplet spectral evolution is represented by decomposition of the actual spectrum into base functions that are produced from the nucleation spectrum through further condensation growth. The proposed scheme is efficient from a numerical point of view, and it allows clearer interpretation of results. In this paper the new approach is discussed, and results of its application to the two-dimensional simulation of small cumulus are presented.

2. The numerical model and setup of the experiment

The numerical model used in this study is a two-dimensional version of the anelastic cloud model of Clark (1977, 1979) combined with the microphysical model designed to predict droplet spectral evolution. Clark's model predicts cloud development based on the bulk approach to the condensation process. The microphysical model calculates the evolution of cloud droplet spectra using the condensation/evaporation rate as predicted by the dynamical model for a given grid location. Sedimentation and coalescence of cloud droplets are not taken into account, and ice particles are not allowed to form.

a. Dynamical model

Since Clark's model has been widely documented in the literature, only a brief description and basic references will be given here. The model approximates the anelastic, nonhydrostatic atmospheric equations with moist thermodynamics using finite differences (Clark 1977, 1979). The second-order accurate scheme, centered in time and space (Lilly 1965; Arakawa 1966), is used for the momentum equations. In the experiments reported herein, the moist thermodynamics is limited to the condensation–evaporation process, and the advection–condensation problem is solved using time splitting (Clark 1979; Grabowski and Smolarkiewicz 1990). The advection algorithm of Smolarkiewicz (1984) with one corrective iteration and with the monotonicity correction (Smolarkiewicz and Grabowski 1990) is used for all thermodynamic variables. The entire model algorithm is second order in time and space (Smolarkiewicz and Clark 1986). The subgrid-scale mixing processes are represented using the first-order closure of Lilly (1962) and Smagorinsky (1963) (see Clark 1977). The current experiment employs two interacting domains (Clark and Farley 1984). The low-resolution outer domain (5 km in the horizontal and 4 km in the vertical, spatial resolution of 50 m) resolves compensating motions in the environment. The inner domain (2 km × 2 km, resolution of 25 m) provides more resolution in the region where cloud forms. The time step used in the experiment is 5 and 2.5 s in the outer and inner domain, respectively. The microphysical model is applied only in the higher-resolution inner domain.

b. Microphysical model

1) Introductory considerations and model assumptions

In a bulk microphysical parameterization, cloud is assumed to be at water saturation; that is, supersaturation required for growth of cloud droplets is not taken into account. The justification for this assumption comes from the observation that a typical value of the supersaturation inside nonprecipitating cloud is small, usually of the order of 0.1% (that is, $q_v/q_{vs} - 1 \sim 10^{-3}$). In regions of nucleation (e.g., near cloud base), a typical value for the supersaturation is about an order of magnitude higher ($\sim$1%), and temperature may deviate from the value predicted by the bulk approach by as much as 0.3 K. Since this difference is compensated after the nucleation, it has a small effect on the overall dynamics of a simulated cloud. The small (on average) value of the supersaturation inside a typical cloud means that almost all water vapor available for growth is actually converted into liquid. Thus, evolution of the cloud droplet spectrum may be approximated assuming that the supersaturation (constant over model time step) is such as to allow condensation of all water vapor available for growth. As far as evaporation of cloud water is concerned, the bulk microphysical model assumes that cloud water evaporates instantaneously and does not consider a finite time required for droplet evaporation. This assumption, especially important for the evaporation caused by mixing between cloud and its environment, will be further discussed later in this section.

Supersaturation plays a crucial role during the activation phase. Total droplet concentration and the size

distribution resulting from the nucleation process (f_0) are determined by the maximum supersaturation reached during nucleation.[2] However, the scale of this process is usually much smaller than the scale resolved by the numerical model. This is especially true in regions of mixing between cloud and its environment, where supersaturation is likely to fluctuate at very fine scales. To simulate the activation process, the model should explicitly represent extremely small scales and use the distribution of unactivated nuclei as a prognostic variable. A simple yet still realistic approach would be to prescribe a family of initial droplet spectra, with the shape of each spectrum being dependent on the CCN distribution and on the (grid-averaged) supersaturation. In the current study, however, an even simpler approach is used: nucleation is parameterized assuming that it always produces the same spectrum, that is, that the distribution of nuclei is uniform below and around the cloud, and that the maximum supersaturation in nucleation regions is always the same. This hypothesis has already been used in Brenguier (1990) based on the observation that total droplet concentration is almost constant despite mixing with environmental air. An additional argument based on the results of the current simulations will be presented later in the paper. It should also be noted that in the current approach nucleation has to be completed within the grid box and the model spatial resolution, Δ, cannot be too fine (say, $\Delta \geq 10$ m).

When droplet sedimentation is neglected, evolution of the cloud droplet spectrum may be calculated using base functions (elementary droplet populations, or EDPs) generated by further condensational growth of the initial spectrum, f_0 (Brenguier 1991). Since only one set of EDPs (those generated from a single initial spectrum f_0) is used in the calculations, the current approach should tend to produce spectra with less variability in terms of position and width of spectral peaks than the approach with various degrees of nucleation. It should also be remembered that numerical dispersion associated with the calculation of droplet growth provides additional broadening of spectral peaks.

The approach proposed in this paper is designed to include effects of entrainment and mixing on cloud droplet spectra. A very simple model of the mixing process for very high Reynolds number flows typical for an atmospheric situation is used as a base for the approach. The model assumes that the time scale for the mixing process (that is, for the homogenization of the volume consisting initially from undiluted cloudy air and droplet-free air) is large and comparable to the time scale of the cloud evolution. This is based on the observation that mixing in the atmosphere requires considerable time to break an initial eddy (of the size of, say, 100 m) into structures with sizes comparable to the Kolmogorov microscale where molecular processes can complete the mixing. As the process of the breakup progresses, the local droplet concentration (i.e., the concentration inside cloudy filaments) should be constant and correspond to the concentration observed just after nucleation. However, concentration observed over the large volume (as compared to the size of the cloudy filament) would be diluted (cf. Paluch and Baumgardner 1989; Brenguier 1990). The evaporation of cloud water as a result of mixing should occur only near the interface separating cloudy and cloud-free air, and it should lead to a decrease of the volume of cloudy filaments. This picture of the mixing process corresponds to that of inhomogeneous mixing (Baker et al. 1980). In this approach the number of droplets per unit mass of air observed over the model grid may be used to distinguish between homogeneous (that is, fully cloudy) and inhomogeneous (that is, partly cloudy) grid volumes; the volume is homogeneous only if the concentration of cloud droplets (per unit mass) is equal to that resulting from nucleation.

As far as phase changes due to vertical displacements are concerned, both condensation and evaporation of cloud droplets inside cloudy filaments are approximated by a homogeneous process; that is, all droplets are assumed to experience the same super- or undersaturation. Thus, in the case of condensation (that is, inside rising parcels), existing droplets homogeneously grow inside cloudy filaments, and nucleation followed by some growth occurs inside initially cloud-free filaments. In the case of evaporation (that is, inside descending parcels), homogeneous evaporation occurs inside cloudy filaments. It follows that the model should take into account both inhomogeneous and homogeneous evaporation for diluted (on the average) air parcels. A very simple approach to realize these two processes simultaneously will be presented in the next section.

The microphysical model built upon assumptions discussed previously represents the simplest possible approach to the problem. For example, neither temperature nor relative humidity differences between cloudy and cloud-free filaments are considered (that is, subgrid-scale structures of thermodynamic variables are not taken into account). Also, parameterization of the nucleation is extremely simple, and, as will become clear in the next section, partition between homogeneous and inhomogeneous evaporation for diluted grid volumes is very arbitrary. More sophisticated formulation of the microphysical model should be considered in the future.

[2] Traditionally, size distributions as f_0 are expressed as number of droplets per unit volume of air and per unit radius interval. Throughout this paper, however, size distributions are expressed as number of droplets per unit mass of air and per unit radius interval, that is, divided by air density. The difference between the two is similar to the difference between concentration (in units of kg m^{-3}) and mixing ratio (kg kg^{-1}). Note that both size distributions per unit mass and mixing ratios are invariant when vertical displacements of an adiabatic parcel in the environment with density stratification are considered.

2) FORMULATION OF THE MODEL

Let $h(\mathbf{x}, r, t)$ be the number of droplets per unit mass of air and per unit size interval, where $\mathbf{x}$ is a position vector, r is the droplet radius, and t is time. When droplet sedimentation is neglected, the conservation equation for $h(\mathbf{x}, r, t)$ may be written in the anelastic system as (e.g., Grabowski 1989):

$$\frac{\partial \rho_0 h}{\partial t} = -\nabla\cdot(\rho_0 \mathbf{u} h) + \nabla\cdot(K\nabla\rho_0 h) - \rho_0 \frac{\partial}{\partial\lambda}\left(\frac{d\lambda}{dt} h\right) + \rho_0 P_h, \quad (1)$$

where $\mathbf{u}$ is the air velocity, λ is a coordinate in radius space that will be chosen, K is the mixing coefficient, P_h is the source term associated with nucleation, and $\rho_o(z)$ is the base-state density of the anelastic system. The first two terms on the right-hand side of (1) represent advection and mixing of cloud droplets, and the third describes condensational growth.

The diffusional growth of a single cloud droplet is approximated as

$$\frac{dr}{dt} = \frac{AS(t)}{r + a}, \quad (2)$$

where S is the supersaturation, a is the length associated with the accommodation coefficient, and $A \approx 10^{-10}$ m^2 s^{-1}. When only condensational growth of a droplet population is considered, the simplified version of (1) becomes

$$\frac{\partial f(r, t)}{\partial t} = -\frac{\partial}{\partial r}\left[\frac{dr}{dt} f(r, t)\right],$$

and the size distribution of an ensemble of droplets following the same trajectory in the cloud (the same history of S) and represented by the distribution f_0 at $t = t_0$, is given by (cf. Brenguier 1991):

$$f(r, t) = f(r, b^2(t)) = f_0(r_0)\frac{r + a}{r_0 + a}, \quad (3)$$

where

$$b^2(t) = (r + a)^2 - (r_0 + a)^2 = 2A\int_{t_0}^{t} S(t^*)dt^*, \quad (4)$$

and r_0 is the initial radius (that is, just after the activation at $t = t_0$) of a droplet with the radius r at time t. The b^2 variable as defined in (4) is used throughout the paper as a coordinate λ in the radius space (that is, $\lambda \equiv b^2$). This gives $d\lambda/dt = 2AS(t)$ in (1), which is independent of the droplet radius.

Equation (3) defines a class of elementary droplet populations, or EDPs $f(r, b^2)$. Each EDP is characterized by its spectrum just after activation (f_0) and its degree of condensational growth (b^2). In this paper, it is assumed that activation produces always the same initial spectrum f_0, and only various degrees of condensational growth are considered. Any actual distribution of cloud droplets can be decomposed using EDPs as follows (Brenguier 1991):

$$h(\mathbf{x}, r, t) = \int \psi(\mathbf{x}, b^2, t) f(r, b^2) db^2 \quad (5a)$$

or in discrete form when a finite number ($=n_c$) of base functions (EDPs) is considered:

$$h(\mathbf{x}, r, t) = \sum_{i=0}^{n_c-1} \psi_i(\mathbf{x}, t) f_i(r), \quad (5b)$$

where $\psi(b^2)$ (or ψ_i in the discrete case) are coefficients of the decomposition, that is, the percentage in an actual distribution of EDPs with a degree of condensational growth b^2. Note that $\psi(\mathbf{x}, b^2, t)db^2$ can also be regarded as the fraction of mass at the grid point at $\mathbf{x}$, at time t, which is characterized by growth parameters in the range b^2 to $b^2 + db^2$.

If only cloudy parcels are advected and mixed, $\int \psi(b^2)db^2 = 1$ (or $\sum \psi_i = 1$), which means that the total droplet concentration per unit mass averaged over the grid is constant and equal to the concentration of activated nuclei: $N_0 = \int_0^\infty h(r)dr = \int_0^\infty f_0(r)dr$. The grid volume for which $\beta \equiv \sum \psi_i = 1$ will thus be referred to as a homogeneous one. When $\beta < 1$, the droplet concentration averaged over the grid is βN_0, that is, smaller than N_0. Since in the current approach local droplet concentration (per unit mass) is always assumed constant and equal to N_0, the grid volume in the $\beta < 1$ case is considered inhomogeneous with the β part of the air mass within the grid box being cloudy and having undiluted local droplet concentration, and the $(1 - \beta)$ part being cloud free.

Using (5a) in (1) leads to the equation for $\psi(\mathbf{x}, b^2, t)$ in the form

$$\rho_0 \frac{\partial}{\partial t}\psi(\mathbf{x}, b^2, t) = -\nabla\cdot[\rho_0 \mathbf{u}^* \psi(\mathbf{x}, b^2, t)] - \rho_0 \frac{\partial}{\partial b^2}\left[\frac{db^2}{dt}\psi(\mathbf{x}, b^2, t)\right] + \rho_0 P_\psi, \quad (6)$$

where $P_h = \int P_\psi f(r, b^2)db^2$ and $\mathbf{u}^*$ is the velocity field that already includes diffusive fluxes (Smolarkiewicz and Clark 1986). In the numerical model (6) is solved using traditional time-splitting technique; that is, time tendency on the left-hand side is written as a sum of two terms describing transport (that is, advection and mixing) of ψ in the physical space $(\partial\psi/\partial t)_{\text{trans}}$ and evolution of ψ due to condensation/evaporation $(\partial\psi/\partial t)_{\text{cond}}$. Transport in the physical space is calculated first. With a finite number of base functions f_i in (5b), the transport part of (6) may be written as

$$\left(\frac{\partial\psi}{\partial t}\right)_{\text{trans}} + \frac{1}{\rho_0}\nabla\cdot(\rho_0 \mathbf{u}^* \psi) = 0, \quad (7a)$$

and must be solved for each ψ_i. The second term $(\partial\psi/\partial t)_{\text{cond}}$, that is, the microphysical adjustment procedure, is then calculated according to:

$$\left(\frac{\partial\psi}{\partial t}\right)_{\text{cond}} + \frac{\partial}{\partial b^2}\left(\frac{db^2}{dt}\psi\right) = P_\psi. \qquad (7b)$$

Values of ψ_i already updated by (7a) are used in (7b). The term P_ψ is either a source when nucleation is occurring or a sink in the case of evaporation. Both the P_ψ term and the logic of the microphysical adjustment procedure associated with (7b) depend upon the homogeneity of the grid box and are discussed in the following. Finite difference techniques used to solve (7) and numerical aspects of the microphysical model will be further discussed in section 2b.

(i) *The homogeneous grid volume.* When $\beta = 1$, the grid box is homogeneous. In this case droplet spectral changes due to condensation or evaporation are calculated assuming that all droplets experience the same supersaturation. The actual value of supersaturation is predicted from the constraint that the amount of water vapor condensed (or evaporated) over the time step, Δq, is that predicted by the bulk model (that is, is equal to the amount required to maintain exact saturation of the grid volume). This is realized by the following procedure. First, the mixing ratio of water condensed for assumed supersaturation S^* (say, $S^* = \pm 0.1\%$ with the sign that depends upon the sign of Δq) is calculated as $\Delta q^* = \sum q_i(\psi_i^* - \psi_i)$, where ψ^* is calculated from ψ using (7b) with $S = S^*$, and q_i is the cloud water mixing ratio associated with f_i. Since the amount of condensate is proportional to supersaturation, the supersaturation that leads to Δq is calculated as $S = S^*\Delta q/\Delta q^*$. This value of the supersaturation is used to calculate the change of droplet spectrum as predicted by (7b). Supersaturation predicted as just described should correspond to the quasi-equilibrium supersaturation resulting from a balance between the source due to vertical motions and the sink due to condensation/evaporation.

(ii) *The inhomogeneous grid volume.* For an inhomogeneous volume ($\beta < 1$), condensation and evaporation scenarios differ. For condensation ($\Delta q > 0$), it is assumed that the β part of the air mass inside a grid box is undiluted and Δq has to condense there. The $1 - \beta$ part of the mass is droplet free, so Δq will result in nucleation and possibly some growth. The initial mixing ratio of cloud droplets in the undiluted part is given by $\psi_i^H = \psi_i/\beta$. (Note that $\sum \psi_i^H = 1$.) Thus, condensation on the undiluted part is performed as in the homogeneous volume but using ψ_i^H. The growth results in ψ_i^{*H}. Only nucleation is performed in the $1 - \beta$ part of the mass when $\Delta q \leq q_0$ (q_0 is the cloud water mixing ratio associated with the nucleation spectrum f_0). Nucleation leads to $\psi_i^{*I} = \delta_{i0}\Delta q/q_0$, where δ is the Kronecker symbol. When $\Delta q > q_0$, nucleation is followed by diffusional growth, as in the homogeneous case with the mixing ratio of water vapor to condense equal to $\Delta q - q_0$ and the initial spectrum defined by $\psi_i^I = \delta_{i0}$. Nucleation followed by some growth leads to ψ_i^{*I} with $\sum \psi_i^{*I} = 1$. The final spectrum in the grid box is defined as $\psi_i^* = \beta\psi_i^{*H} + (1 - \beta)\psi_i^{*I}$. This procedure ensures that the average increase of cloud water mixing ratio defined as $\sum q_i(\psi_i^* - \psi_i)$ is exactly equal to Δq. Note also that the initially inhomogeneous grid volume may became homogeneous as a result of fresh nucleation on the initially droplet-free part.

For evaporation ($\Delta q < 0$) over an inhomogeneous volume ($\beta < 1$), the mixing ratio that has to evaporate on the cloudy β part of the grid box is $\Delta q/\beta$ in order to produce the required grid-averaged evaporation. To allow both homogeneous and inhomogeneous evaporation, the following procedure is adopted. In a δ portion of the cloudy air ($0 \leq \delta \leq 1$), droplets evaporate homogeneously, that is, they are all exposed to the same subsaturation with the mixing ratio of water substance subject to phase change equal to $\Delta q/\beta$. This is represented using $\psi_i^H = \psi_i/\beta$ and the same procedure as for the condensation results in ψ_i^{*H}. In the rest of cloudy air [$\beta(1 - \delta)$], extremely inhomogeneous evaporation is assumed to occur: in some small volumes droplets evaporate totally, and in others they do not evaporate at all. In such a process, average spectra before and after adjustment are related via the formula $\psi_i^{*I} = \epsilon\psi_i^I$, where $\psi_i^I = \psi_i^H$ and ϵ is defined by the mixing ratio of cloud water that has to evaporate: $\epsilon = (q_c^m + \Delta q)/q_c^m$, where $q_c^m = \sum \psi_i q_i$ is the cloud water mixing ratio inside the grid box prior to evaporation. The final spectrum in the grid box is defined as $\psi_i^* = \beta[\delta\psi_i^{*H} + (1 - \delta)\psi_i^{*H}]$. Again, such a procedure ensures that the change of cloud water mixing ratio $\sum q_i(\psi_i^* - \psi_i)$ is exactly equal to Δq.

To complete the formulation of the microphysical model, the parameter δ introduced above must be specified. Note that $\delta = 1$ gives only homogeneous evaporation and $\delta = 0$ results in only inhomogeneous evaporation. As discussed in the previous section, δ should depend primarily upon the ratio between the amount of cloud water subject to evaporation due to descending motions and the amount due to mixing. Unfortunately, this information is not easily available from the bulk model. An additional complication important at this point is that the amount of water substance subject to phase change as predicted by the bulk model may significantly differ from the amount predicted when the subgrid-scale structure of thermodynamical fields is taken into account. Because of these uncertainties, a very simple formulation for δ is adopted in the current study and it is assumed that $\delta = \beta$. This formulation gives only homogeneous evaporation in the case of homogeneous volume (that is, no mixing) and a compromise between homogeneous and inhomogeneous evaporation for the case of inhomogeneous volume. In the authors' opinion, the actual parame-

terization of δ has small effect on the very general aspects of droplet spectral evolution discussed in this paper.

The nucleation spectrum f_0 used in calculations reported herein is chosen as in Brenguier (1991), that is, $f_0(r_0) = k/r_0^{\gamma+1}$ for $r_0^- \leq r_0 \leq r_0^+$ and $f_0(r_0) = 0$ otherwise, where $k = N_0\gamma/[(r_0^-)^{-\gamma} - (r_0^+)^{-\gamma}]$, $N_0 = 10^3$ mg^{-1} (that is, 10^3 cm^{-3} for the air density of 1 kg m^{-3}), $\gamma = 3$, $r_0^- = 1$ μm, and $r_0^+ = 15$ μm.

3) Numerical aspects of the microphysical model

In the current experiments $n_c = 30$ EDPs in the b^2 space are used. They are linearly distributed from $b^2 = 0$ up to $b^2 = (r_{\max} + a)^2 - (r_0^- + a)^2$ with $r_{\max} = 12$ μm. Also, $a = 2$ μm is assumed. In each time step microphysical calculations begin with the calculation of $(\partial\psi/\partial t)_{\text{trans}}$ in (7a) using the second-order monotone scheme of Smolarkiewicz and Grabowski (1990). Next, adjustments associated with $(\partial\psi/\partial t)_{\text{cond}}$ are performed according to the logic previously described and the fully third-order scheme of Smolarkiewicz (Margolin and Smolarkiewicz 1989) is used in (7b). To ensure consistency between dynamical and microphysical models and the consistency of the microphysical model itself, the actual calculations in the adjustment step proceed in the following way. First, a correction is applied to the advected ψ_i^a at each grid location to ensure that $\sum \psi_i^* = \beta^a$, where the superscript a refers to the solution of (7a) and * refers to the corrected value. [Note that this requires (7a) to be solved with $\beta = \sum \psi_i$.] The correction is performed as $\psi_i^* = \alpha\psi_i^a$ with $\alpha = \beta^a/(\sum \psi_i^a)$. The procedure leads to only minor modification of the ψ_i field: α is usually equal to one within a very small error. Next, the adjustment associated with droplet growth/evaporation is performed to ensure that $\sum \psi_i^f q_i = q_c$, where ψ_i^f is the final value of the ψ_i at a given grid location [that is, after applying time tendencies due to (7a) and (7b)], and q_c is the already adjusted cloud water field from the bulk dynamical model. Thus, the amount of water substance subject to the phase change that is used in the microphysical adjustment scheme is $\Delta q = q_c - \sum \psi_i^* q_i$.

c. *Environmental sounding and cloud forcing*

The idealized thermodynamic sounding used in the experiment described in this paper and the adiabatic parcel analysis for this sounding are presented in Fig. 1. The sounding[3] is characterized by moist and stable air up to the inversion at about 1.8 km that limits cloud development. Across the inversion the humidity drops from about 90% to about 50% and continues to decrease with height above the inversion. The cloud base for the adiabatic parcel rising from the $z = 0$ level is at about 450 m and the cloud top (defined here as the zero buoyancy level) is slightly above the inversion, roughly at 2 km. To initiate the cloud, a convergence zone is introduced at the lowest 0.7 km, centered in the middle of the domain. The analytic form of the streamfunction associated with the convergence zone was chosen (M. Moncrieff, personal communication) as:

$$\Psi^* = z^*(z^* - 1) + \left(\frac{2}{\pi}\right)^3 \sum_{m=0}^{\infty} \frac{\sin[(2m+1)\pi z^*]}{(2m+1)^3} \times \exp[-(2m+1)\pi x^*] \quad (8)$$

for the right-hand half of the domain and $-\Psi^*$ in the left-hand half. In (8) dimensionless variables are defined as $z^* = z/H$, $x^* = (x - x_c)/L$ (where x_c is the center of the domain), and $\Psi^* = \Psi/(Hw)$. In the current experiment $H = 0.7$ km, $L = 1.5$ km, and $w = 6$ m s^{-1}. Except for the flow associated with the convergence zone, the atmosphere has been assumed to be initially at rest.

3. Results

a. *General features of the bulk model results*

Figure 2 presents fields of vertical velocity, water vapor mixing ratio, and the outline of a cloud at $t = 10$ min for the outer domain to show the overall geometry of the experiment. The superimposed low-level convergence produces a narrow updraft with a peak velocity of about 2 m s^{-1} that lifts the air up to the condensation level at height of about 500 m. Figures 3 and 4 show the cloud water mixing ratio and a vertical velocity between 18 and 34 min for the inner domain. Apparently, the convergence allows the boundary-layer air to reach a level of free convection (at about 900 m, see Fig. 1) from which the cloud rises with peak updrafts increasing from about 3 m s^{-1} at $t = 18$ min up to about 8 m s^{-1} at $t = 34$ min. The interaction of the cloud updraft with the inversion and dry overlying air produces complex updraft–downdraft structures in the upper part of the cloud. At $t = 30$ min the upper part of the cloud seems to represent a mixture of the cloud material arriving at the inversion at different times and the environmental dry air. The lower part of the cloud is affected by mixing only near cloud edges.

The rest of the paper is devoted to an analysis of the cloud droplet spectra and physical processes responsible for their development in the model-generated cloud. Before that, however, a comparison between the b^2 spectrum and the traditional spectrum in the radius space will be discussed. Also, the format of plots with microphysical data used in the rest of the paper will be presented.

[3] This idealized sounding has a structure similar to soundings taken off the coast of Hawaii (Raga et al. 1990). Clouds that develop in this environment have a maritime character and precipitate heavily. The reason for using this particular sounding for a microphysically unrealistic situation is that the sounding and the cloud forcing mechanism provide a simple yet interesting dynamical framework in which microphysical interactions may be discussed.

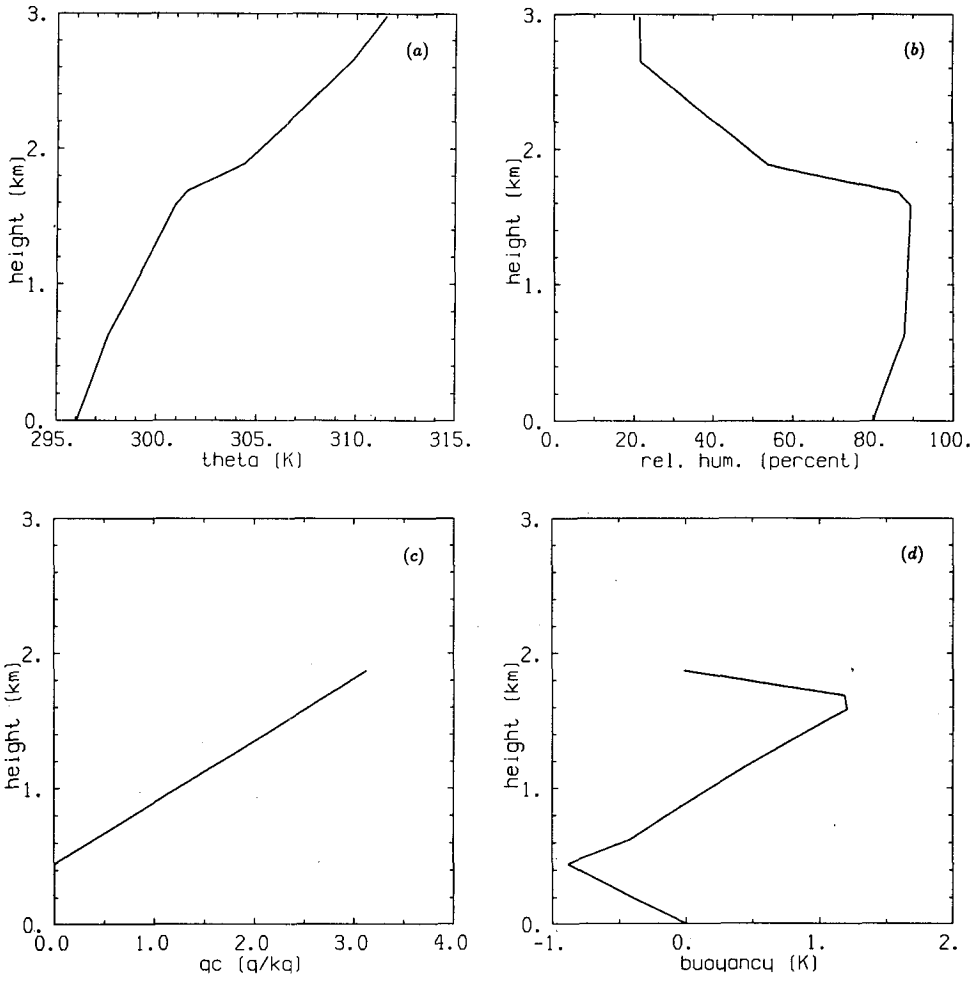

FIG. 1. Environmental potential temperature $\bar{\theta}$ in (a) and relative humidity $100\bar{q}_v/q_{vs}(\bar{\theta})$ in (b) as a function of height. Cloud water mixing ratio q_c in (c) and buoyancy $B = \theta - \bar{\theta} + \bar{\theta}[0.61(q_v - \bar{q}_v) - q_c]$ in (d) for an adiabatic parcel rising from $z = 0$ level.

b. Size distribution and b^2 distribution

In the b^2 scheme, each spectrum is developed as a combination of EDPs, characterized by different values of b^2. An EDP is made of droplets that followed the same trajectory in the cloud, and b^2 is proportional to the integral of supersaturation along this trajectory. Therefore, the b^2 distribution in a given grid volume describes the proportion in a spectrum of droplets of different sizes having experienced the same amount of diffusional growth. Figure 5 shows the b^2 distribution $\psi(b^2)$ (solid line) and the corresponding size distribution $h(r)$ (dashed lines). As indicated on the upper right grid box, the intersection of the vertical bar with the x axis marks the adiabatic b value at that level, b_a. Along this bar, the horizontal mark indicates the value q_c/q_c^a (liquid water mixing ratio normalized by the adiabatic liquid water mixing ratio) from 0 at the bottom (x axis) to 1 at the top of the vertical bar. The upper number in the upper right corner of each box is the parameter β that characterizes the grid homogeneity. The lower number is the percentage p of condensation nuclei from the boundary layer. This parameter, which is plotted only in this figure, will be discussed in the next section. By observing a spectrum, it is difficult to evaluate, for example, the proportion of newly activated droplets or proportion of droplets from cloud base, even if an adiabatic spectrum is drawn as a reference. The b^2 distribution immediately depicts these aspects. Activation is characterized by $b = 0$, an ensemble of droplets growing adiabatically from cloud base is identified by the vertical bar at $b = b_a$, and superadiabatic growth is represented by the proportion of b values larger than b_a. Therefore, only b^2 distributions will be shown in the remainder of the paper.

c. Evolution of cloud droplet spectra

After 18 minutes of simulation (Figs. 3 and 4), the cloud has developed a well-organized vortex ring circulation (or, rather, vortex-pair circulation in the two-dimensional case) near cloud top with typical bubble-

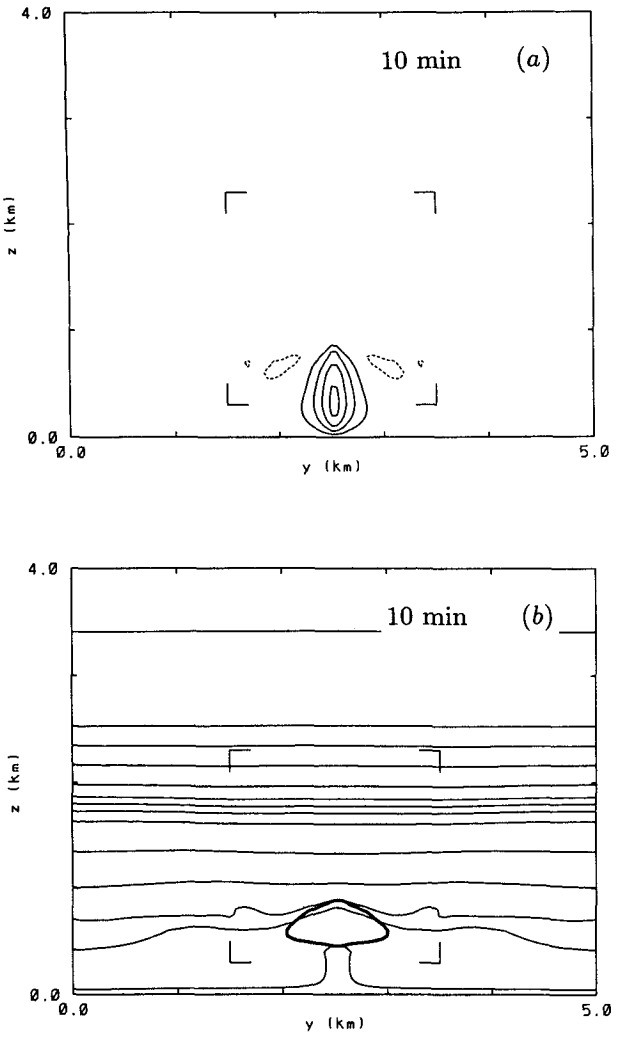

FIG. 2. Vertical velocity (contour interval of 0.5 m s^{-1}; solid and dashed lines are for positive and negative values, respectively) in (a). Water vapor mixing ratio (thin solid line, contour interval of 1 g kg^{-1}) and cloud outline (thick solid line) in (b). Data from the outer domain at t = 10 min. Position at the inner domain is also shown.

like structures. Figure 6 shows the b^2 distributions (6a) and the velocity field (6b) on the left-hand side of the cloud (cell A in Fig. 3a) for t = 18 min. The majority of b^2 distributions are narrow and centered around the adiabatic value, except at the interface between the cloud and its environment. The narrowest distributions illustrate the effects of numerical dispersion on calculations of droplet growth using the b^2 scale. Nucleation, characterized by a high proportion of small b values, occurs on both sides of the updraft at the bottom of the vortices (Fig. 6a), where mixtures of environmental air and cloudy air are entrained in the updraft core (e.g., in the region of x around 2400 m and z between 900 and 1000 m). Note also how the ratio q_c/q_c^a changes across regions of entrainment (e.g., along z = 950 m). In addition, some nucleation occurs at cloud top where cloudy air mixes with the environment. This mixed air, almost free of droplets and with very low ratio of q_c/q_c^a, reaches saturation when it is pushed upward, and new nuclei are activated.

Four minutes later, at t = 22 min, a second vortex has been formed on the upper left-hand side of the cloud, V2 in Fig. 7b. Note that the circulation in vortex V2 has the opposite sign than in vortex V1. The two vortices are separated by the downdraft (with vertical velocity up to -2 m s^{-1}, Fig. 4c) that produces strong dilution: along the downdraft β is typically 0.5 and the ratio q_c/q_c^a is low. Two activation regions have appeared in ascending parts of these vortices (at x = 2375 m, z = 1150 m; and at x = 2075 m, z = 1300 m). The resulting bimodal b^2 distributions (Fig. 7a) are made of droplets ascending from cloud base (the mode at b_a) and droplets growing from the secondary activation level. In the lower right vortex (V1), these small droplets are growing adiabatically, and the corresponding mode increases continuously from the activation level at z = 1150 m to the top of the vortex about 200 m above. On the contrary, in the upper left vortex (V2), mixing with the downdraft has been efficient, the entrained air is drier, and dilution is significant ($\beta < 0.5$ at the base of the vortex). Vertical lifting is not sufficient for activation of all the nuclei on the left-hand side of the vortex ($\beta < 1$), and the mode corresponding to newly activated droplets remains close to $b = 0$. Also, interaction of the rising part of vortex V1 (which already contains bimodal spectra) with the downdraft leads to trimodal spectra in few locations (e.g., around x = 2350 m and z = 1350 m).

This simulation shows that for such small cloud (1 km in diameter), the vortex structure at cloud top is efficient for a broadening of the spectrum. Initially, the cloud is characterized by a simple vortex structure, adiabatic spectra can be observed up to cloud top, and mixing followed by nucleation is restricted to the upper boundary and the bottom of the vortex. Four minutes later the main structure splits in two smaller vortices, and broad multimodal spectra are observed. In general, air both from above the cloud (vortex V2) and from the side of the cloud (vortex V1) is brought into the cloud at this stage.

As time progresses, more air is lifted from the boundary layer, and new bubblelike structures are formed near cloud top. The old structures are being pushed aside by the cloud-scale circulation while the upper part of the cloud is continuously fed by the low-level cloud and the main updraft tilts and stretches. During this evolution, nucleation occurs at the main entrainment level located at the base of the entraining vortex, which is slowly moving with time. For example, at t = 18 min (Fig. 6a), entrainment occurs on both sides of the cloud at the level z = 0.9 km and moves to z = 1.15 km, on the left-hand side, in about 4 minutes (Fig. 7a). This motion is not significant compared to the vertical airspeed in the updraft. Also, the height of the cloud top rises slowly, roughly at the rate of 1

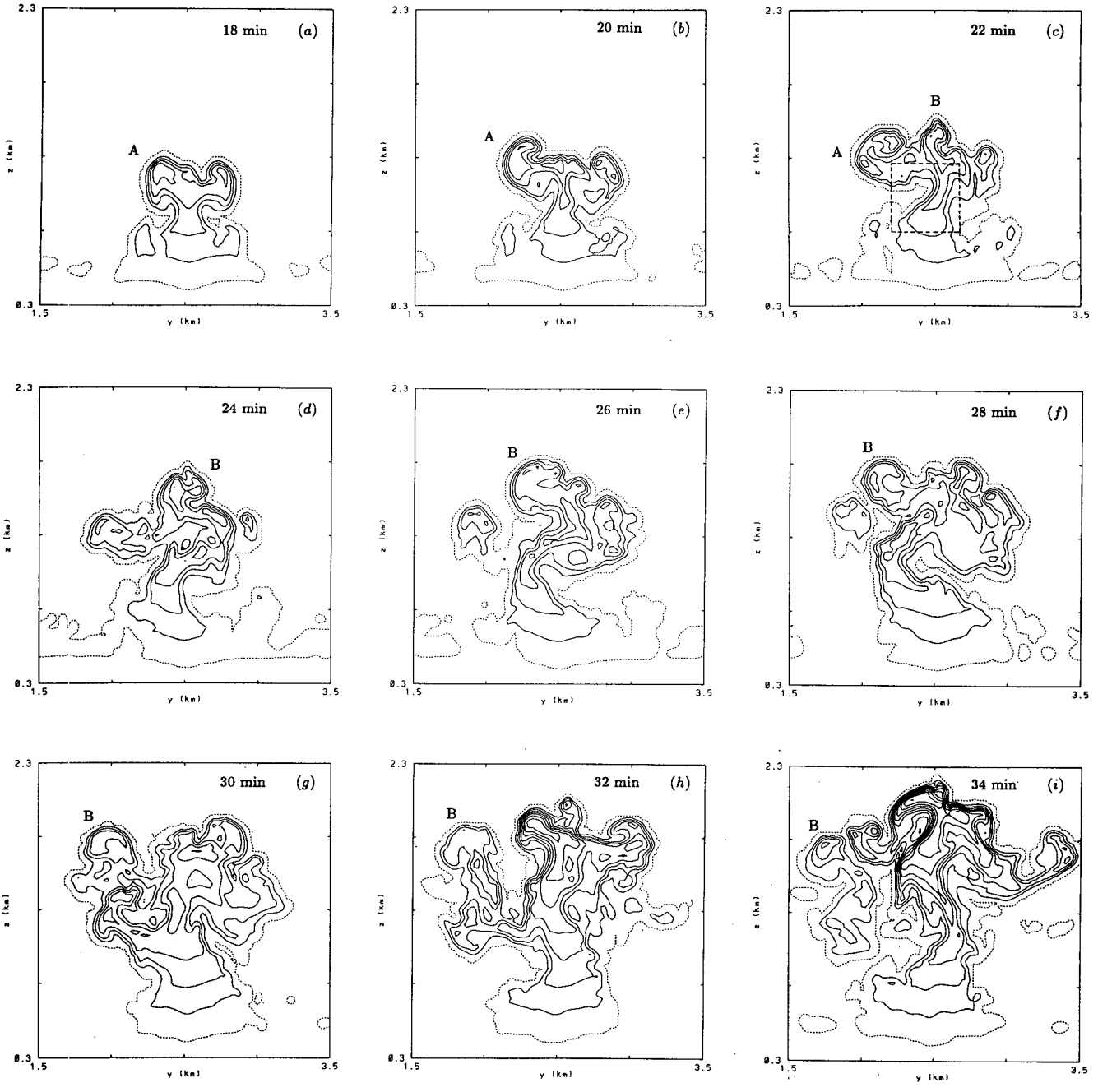

FIG. 3. Cloud water mixing ratio in the inner domain for t = 18 min (a) through t = 34 min (i). Contour interval of 0.4 g kg^{-1}. Dashed line is for mixing ratio of 0.01 g kg^{-1}. Position of the domain shown in Fig. 9 is indicated in (c).

m s^{-1}. Thus, the general mechanism of the spectral broadening (which involves lateral entrainment at lower levels and cloud-top entrainment near the top) remains the same in dynamically active regions. For the side entrainment, it follows that, typically, droplet spectra are made of droplets from cloud base ($b = b_a$) mixed with droplets from a single entrainment level, that is, with a b value ($b < b_a$) that increases as the vertical distance from the entrainment level increases. The updraft is strong enough for complete activation in entrained parcels, so that cloudy air is homogeneous ($\beta = 1$). For entrainment from above the cloud top, the situation is usually more complex and involves a sequence of evaporation (in the downdraft part of a vortex) and reactivation (in the updraft part) for some of cloud droplets. These aspects are nicely represented in Figs. 6 and 7.

Complex b^2 distributions can be observed in old cells, detached from the main updraft by cloud-scale circulation. Such distributions indicate that droplets

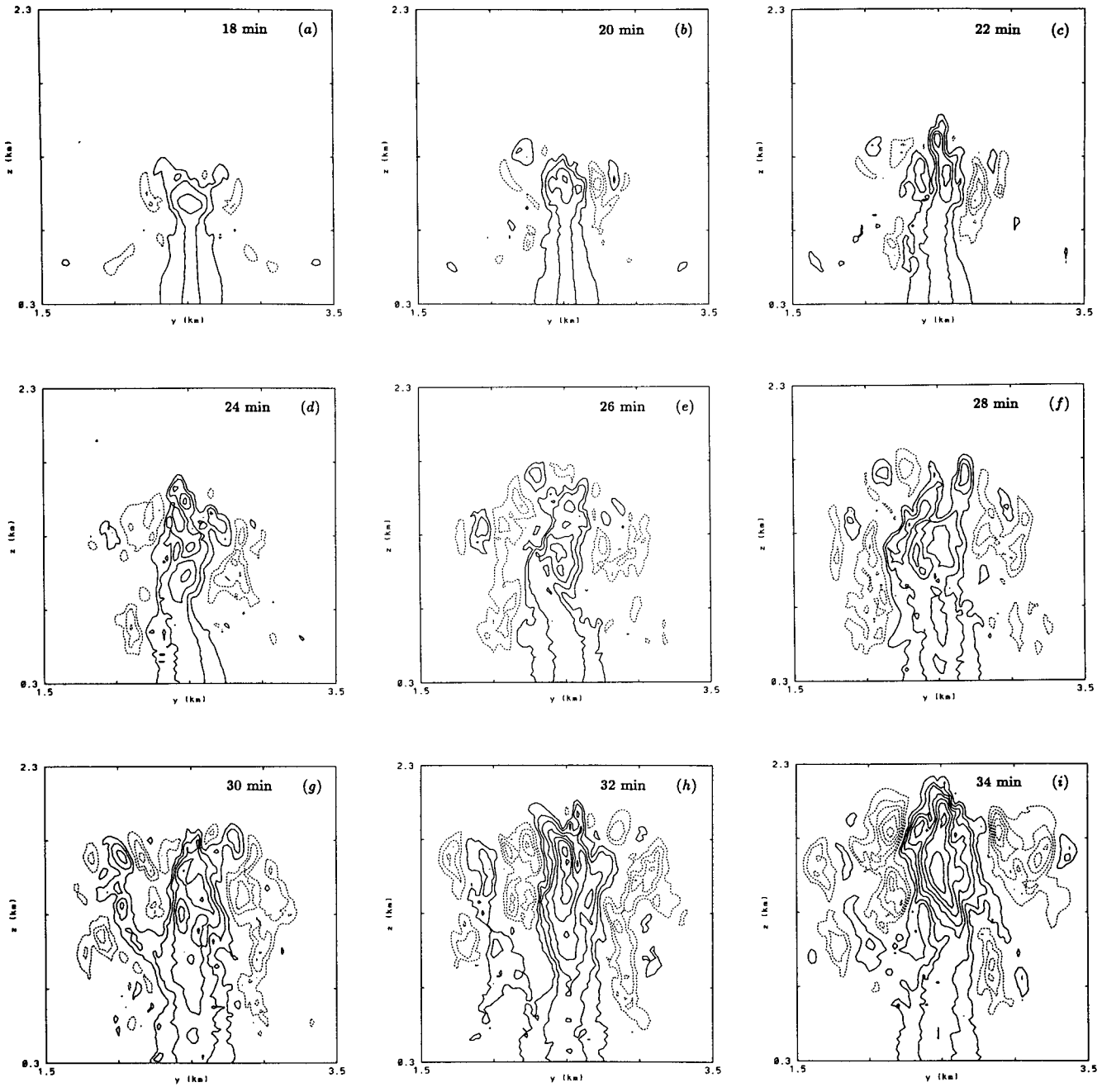

FIG. 4. As in Fig. 3 but for vertical velocity. Contour interval of 1 m s^{-1}. Solid and dashed lines for positive and negative values, respectively, and zero contour is not shown.

characterized by various degrees of condensational growth are mixed at the same level. Figure 8 presents cell B (see Fig. 3) at $t = 34$ min. This cell appeared at $t = 22$ min at cloud top (Fig. 3c). It was forced toward the side by the cloud-scale circulation, separated from the main updraft by a downdraft (Figs. 3g, 3h), and has begun to decay. Within the vortex associated with this cell several types of spectra (both broad and narrow, monomodal and multimodal) can be observed. Parameter β is almost everywhere smaller than 1 so when condensation occurs, new nuclei are activated ($b = 0$) while previously nucleated droplets are growing. Note that the ratio q_c/q_c^a is small, around 0.3 on average, so cloud dilution is significant. Also, a superadiabatic growth of large droplets may be observed at some locations (e.g., around $x = 1750$ m and $z = 1750$ m).

The amount of water vapor to condense on an inhomogeneous grid box is always divided into two parts: one part leads to growth of existing droplets in the

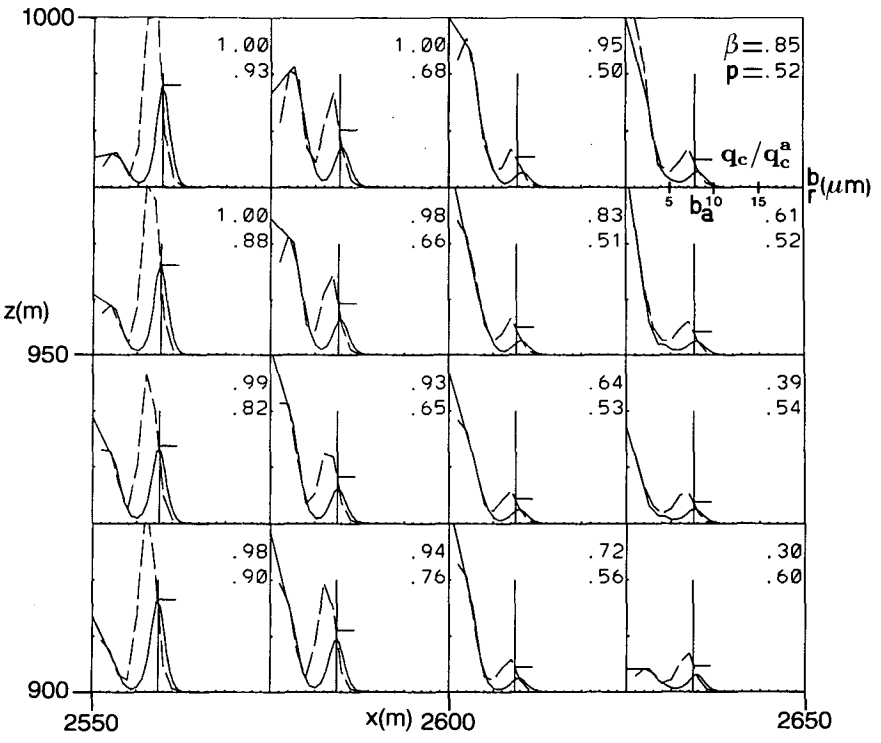

FIG. 5. The b^2 distributions [$\psi(b^2)$, solid lines] and size distributions [$h(r)$, dashed lines] at $t = 22$ min. Position of the domain is indicated in Fig. 9. The intersection of the vertical bar with the x axis is the adiabatic b value (b_a). The horizontal mark on the vertical bar indicates the ratio between the observed cloud water mixing ratio and the adiabatic one. The upper number in the upper right corner is the parameter β that represents the grid homogeneity. The lower number, used only in this figure, is the parameter p that represents the percentage of nuclei from the boundary layer.

cloudy volume (where local droplet concentration is constant and equal to that on the homogeneous grid), and the second part leads to activation of new droplets on the initially droplet-free volume. Such a scheme prevents any additional droplet growth due to a reduction of droplet concentration, which is a traditional explanation of the enhanced (or superadiabatic) growth. Superadiabatic b^2 values produced by the current scheme do not result from smaller local droplet concentrations, but are a direct consequence of the fresh activation. In the current formulation, the mean droplet radius observed on the cloudy volume containing recently activated droplets is smaller as compared to the adiabatic narrow spectrum, and higher quasi-equilibrium supersaturations are possible. Of course, the overall effect depends on the history of all EDPs present in the grid box. The conditions for the maximum superadiabatic growth have been discussed in Brenguier (1990) for a simplified one-dimensional model and examples with the EDP formulation were presented in Brenguier (1991).

4. Discussion

Preliminary analysis illustrates the suitability of this new approach for numerical simulation of the droplet spectral evolution in nonprecipitating cumulus. The b^2 distribution and the size distribution differ, but Fig. 5 shows that they are similar enough for an easy transposition from b to r scales. If the spectrum at nucleation f_0 is known, by analyzing measurements at cloud base or in other activation regions, it is in fact possible to derive a b^2 distribution from a measured spectrum (Brenguier 1991). For analysis of numerical results or experimental data, b^2 distributions are more suitable than spectra because b values are directly related to the degree of condensational growth. This allows predictions of the origins of the various ensembles of droplets composing the examined spectrum. From the numerical point of view, this scheme improves growth calculations without increasing the number of variables. For example, in the present calculations, b values range from 0 to 13.6 μm while droplet sizes range from 1 to 19.8 μm. For the same resolution in size, 41 size classes would be needed instead of the 30 b^2 classes used here.

Since Mason and Chien (1962), the effect of entrainment on vertical evolution of droplet spectra has been frequently described as the result of continuous mixing of cloudy air from cloud base with environmental air entrained through the sides (e.g., Warner 1973; Mason and Jonas 1974). In these models, en-

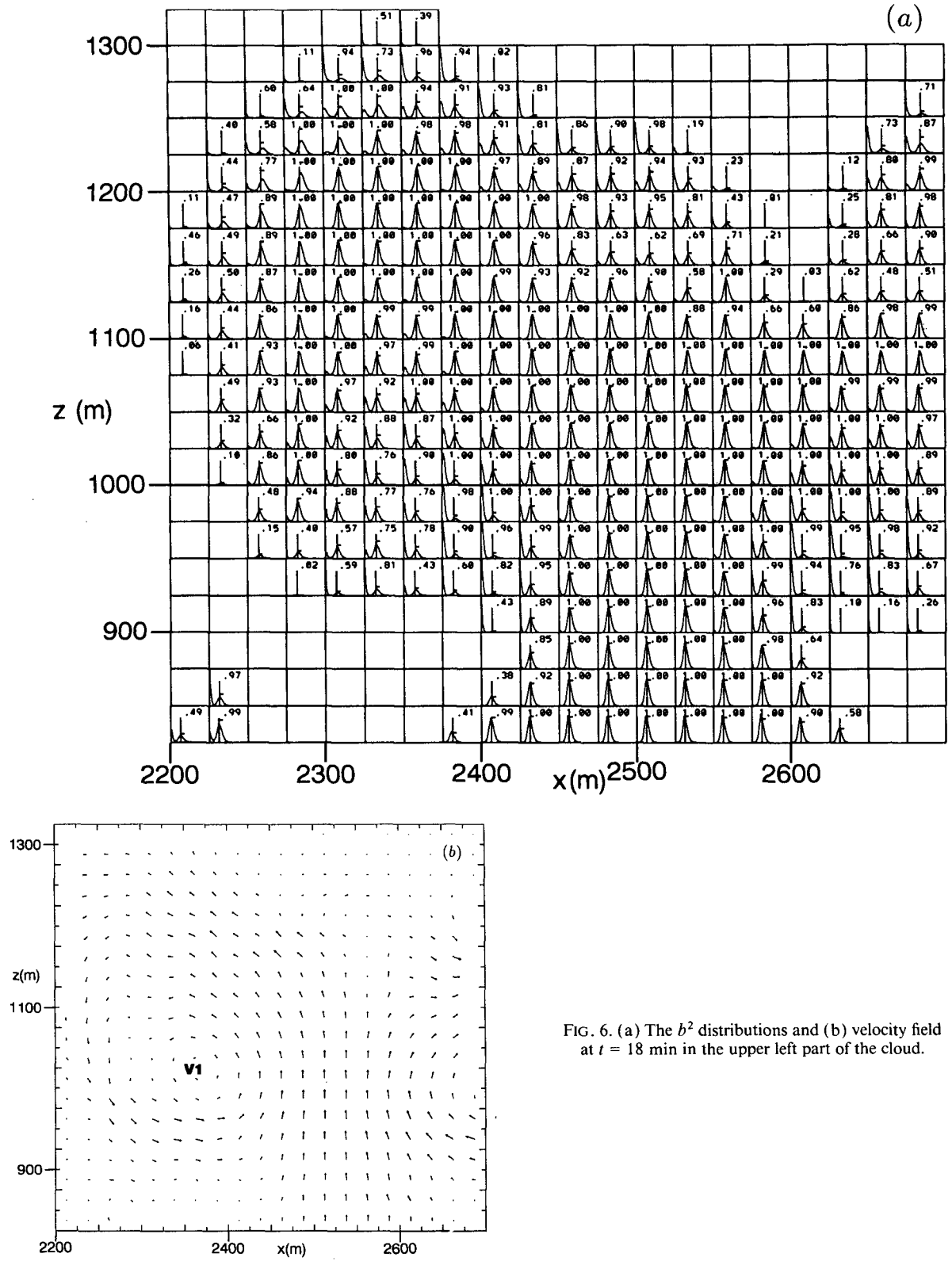

FIG. 6. (a) The b^2 distributions and (b) velocity field at t = 18 min in the upper left part of the cloud.

trained air was assumed to be instantaneously mixed with cloudy air at the entrainment level. Later, Baker et al. (1980) introduced the concept of inhomogeneous mixing, by showing that total evaporation of some cloud droplets is occurring before mixing is completed. Brenguier (1990, 1991) has shown, by a formal study

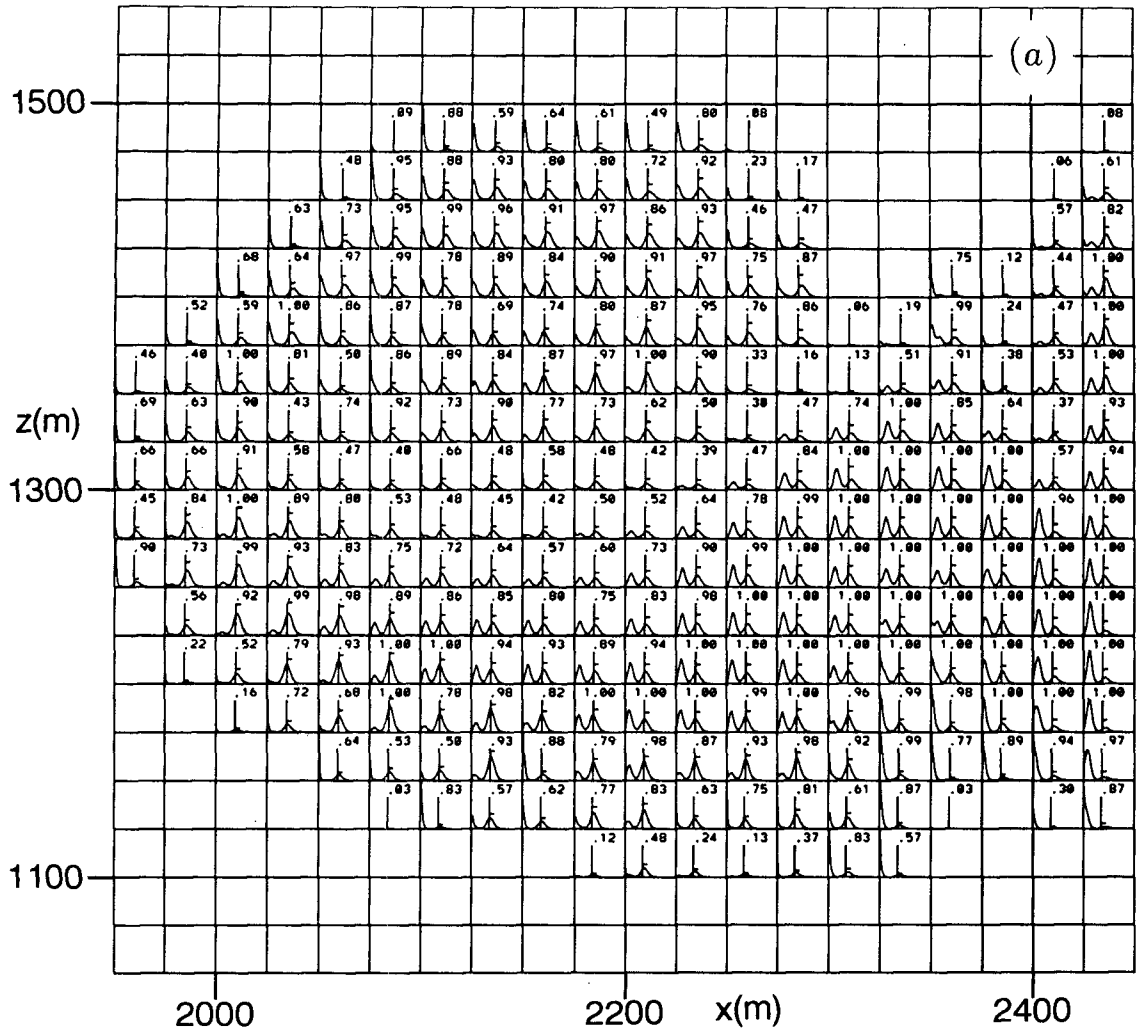

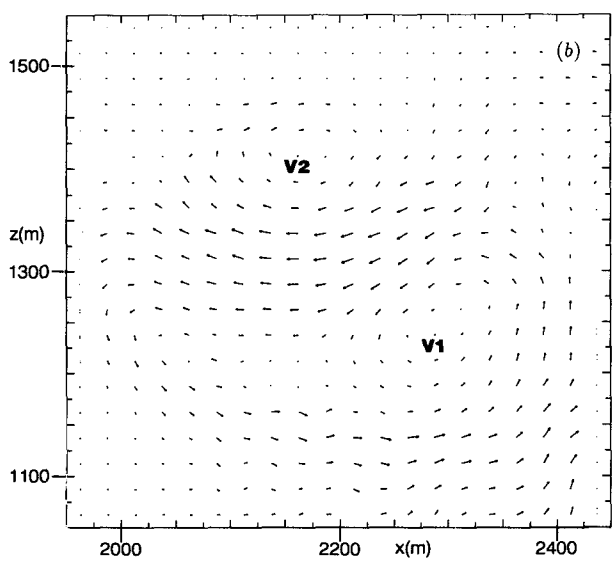

FIG. 7. As in Fig. 6 but at t = 22 min.

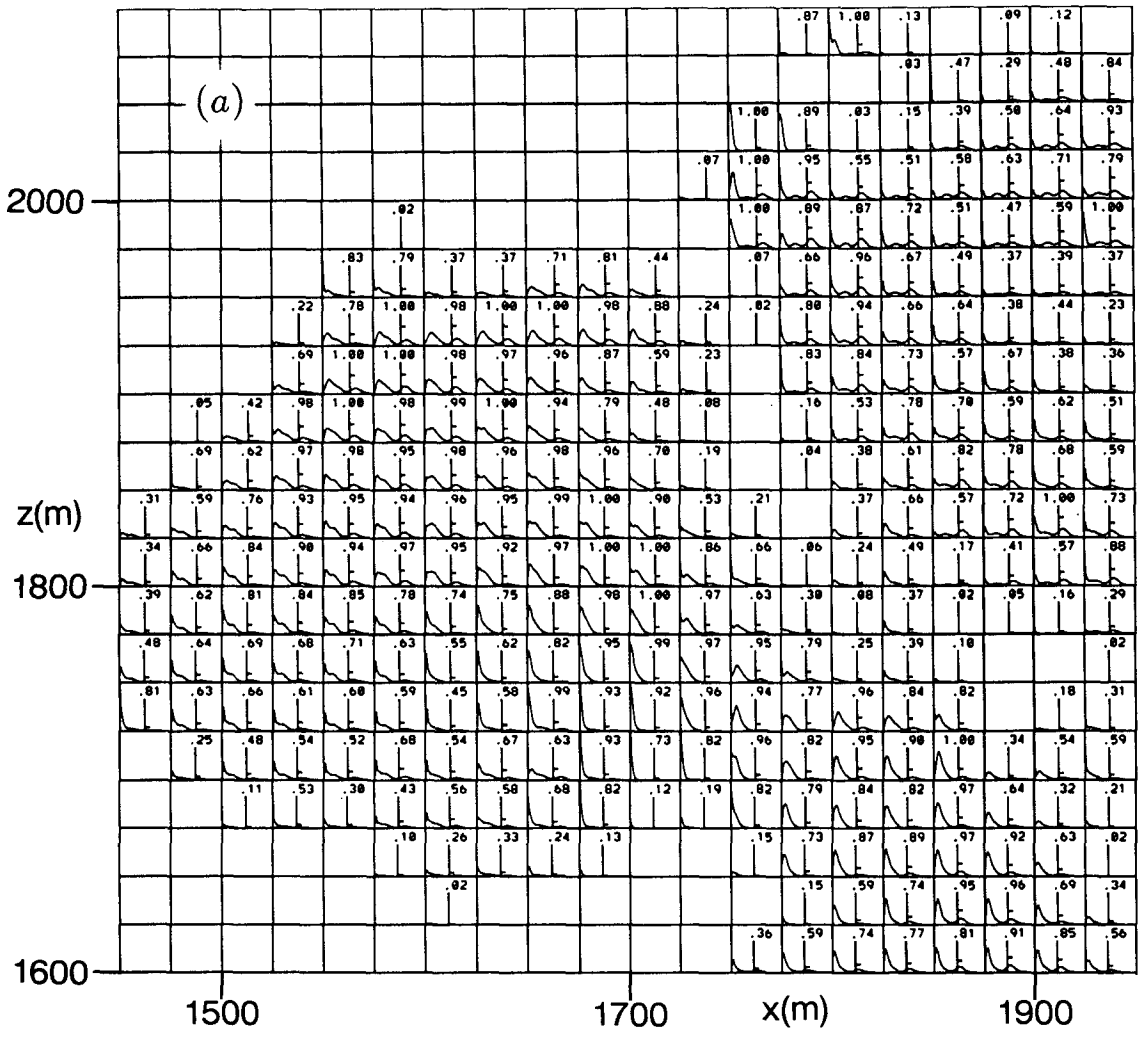

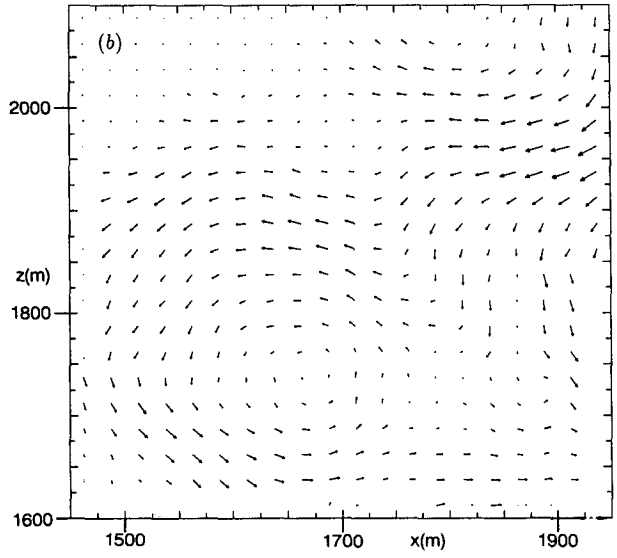

FIG. 8. As in Fig. 6 but at t = 34 min.

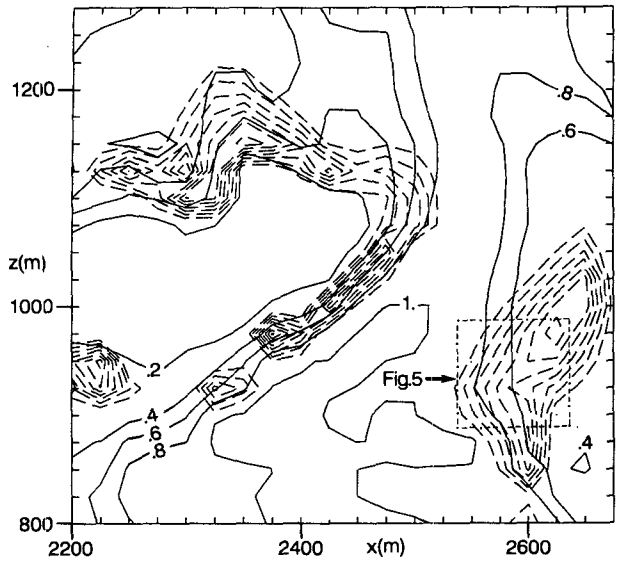

FIG. 9. Field of the parameter p (percentage of nuclei from the boundary layer) from 0.2 to 1 (solid lines, contour interval of 0.2) and field of ψ_0 (proportion of droplets with $b = 0$) from 0.1 to 0.4 (dashed lines, contour interval of 0.05) at $t = 22$ min. The location of the domain is shown in Fig. 3c.

of the continuous entrainment hypothesis, that continuous mixing produces droplet spectra characterized by a narrow mode at a radius corresponding to adiabatic growth from cloud base and a very broad mode at smaller radii (see Figs. 4, 5, and 6 in Brenguier 1991). In the numerical experiment presented here, very few spectra exhibit this pattern. Most of them are either monomodal or bimodal with a mode corresponding to adiabatic growth from the cloud base and an additional mode at b value intermediate between 0 and b_a resulting from the entrainment. Spectra in older, dynamically less active cloud volumes are often highly variable in space and show complex structures, sometimes resembling those generated with the continuous entrainment hypothesis. Spectra typical for continuous entrainment would be observed throughout cloud only if the updraft were able to develop many interacting vortexlike structures such that environmental air entrained at various levels could be finally mixed. However, cloud dynamics does not allow such an evolution in this experiment.

The fundamental aspect of the microphysical model discussed in this paper is the ability to provide fresh nucleation in parcels entrained into actively growing cloud. Fresh nucleation as a result of entrainment has been considered in theoretical studies (e.g., Warner 1969b, 1973) and has been suggested recently using observational data (Paluch and Knight 1984; Bower and Choularton 1988; Stith and Politovich 1989). Fresh nucleation in the microphysical model is a direct consequence of the inhomogeneous mixing between cloudy and cloud-free air; that is, it results from the coexistence of the undiluted cloudy filaments (in which droplets grow) and cloud-free filaments (where nucleation occurs) in air parcels entrained along the updraft. It should be stressed, however, that lack of the subgrid-scale variability of temperature and relative humidity over an inhomogeneous grid volume considerably simplifies the physics of this process. It is not clear what effects these simplifications have on predicted droplet distributions. In general, the microstructure of a cumulus cloud (especially within a region that underwent some mixing) is a controversial issue and contradictory results exist in the literature (e.g., Austin et al. 1985; Paluch and Baumgardner 1989; Baker 1991). Clearly, more research is required in this area.

Cooper (1989) has suggested that spectral broadening can be produced by variable droplet paths through the turbulent field inside a cloud and that special dynamical scenarios and evaporation on small scales are not required. Srivastava (1989), on the other hand, pointed out inconsistencies between definitions of large-scale and microscale supersaturations (with the former resulting from a balance between vertical motions and growth of *droplet population* and the later determining the growth rate of *a single droplet*), which may lead to the broadening of the spectrum. These effects have not been included in the current formulation, and simulated spectra remain narrow in the main updraft until mixing with newly activated droplets become significant. Experimental studies are now needed to corroborate these suggestions. If spectra observed in the main updraft are broader than adiabatic spectra, it might be necessary to expand the current approach and introduce an additional scheme to depict broadening as described by Cooper (1989) or Srivastava (1989).

In numerical models developed for studies of the condensation process, it is generally assumed that the distribution of condensation nuclei is uniform throughout the whole cloud depth [see Brenguier (1990) for a review of previous one-dimensional schemes]. This assumption looks questionable since it has been shown that the concentration of condensation nuclei generally decreases with increasing height over continents (Pruppacher and Klett 1978). However, the cloud itself transports nuclei from the boundary layer, and it is possible that as a result of mixing with the environment these nuclei form a shell around the cloud. If this is the case, nuclei distribution in activation regions might be similar to distribution in the boundary layer. To test this hypothesis, an additional variable p has been introduced in the calculation and processed as a passive scalar with the initial condition (at $t = 0$) of $p = 1$ in the boundary layer and $p = 0$ above. Figure 9 shows part of the whole cloud (shown in Fig. 3c) at $t = 22$ min. This figure presents the p field together with ψ_0 field which is the proportion, in a spectrum, of EDP characterized by $b = 0$. Therefore, ψ_0 is a good indicator of nuclei activation. It appears that nucleation occurs in regions with p between 0.2 and 0.8 (0.5 on average). Details are shown in the previously discussed

Fig. 5, whose location is indicated in Fig. 9 by a dotted square. In the region of activation, p values are larger than 0.5. It follows that, at secondary activation levels, nuclei distributions are determined as much by the distribution in the boundary layer as by distribution above. It also follows that the air entrained into the cloud may have different thermodynamical structure than environmental air at a given level.

Finally, it must be stressed that the results presented in this paper do not represent generalizations on the role of entrainment on droplet spectra in convective clouds. Two-dimensional geometry, low spatial resolution, highly idealized environment (e.g., no shear), and simple cloud-forcing mechanism are major assumptions of this experiment. From the microphysical point of view, the most important limitation is always undiluted local concentration of cloud droplets. As discussed, this seems to be quite a controversial assumption, and it is especially questionable for old cloud volumes where there might be enough time to complete the mixing process. Once the mixing is completed, spectral evolution would follow differently than predicted by the current model; for example, growth of the diluted droplet population without fresh nucleation of cloud droplets would take place in the case of further ascent of a completely mixed (diluted and homogenous) cloudy parcel. Another model limitation results from the restricted number of b^2 classes. In the adiabatic updraft, for example, the mode is not as narrow as it should be only because of numerical dispersion. However, this aspect is not crucial when considering the crudeness of the parameterization used for activation. As far as activation is concerned, the main parameter, that is, water vapor supersaturation, cannot be precisely calculated unless the physics of mixing between cloudy air and clear air (that is, the presence of small-scale structures) is correctly parameterized. The b^2 scheme is especially appropriate for this kind of parameterization since fluctuations of maximum supersaturation in activation regions can be related to a single parameter: the size of the smallest activated nucleus (Brenguier 1991). Some of the issues previously discussed suggest improvements to the microphysical model and such work is planned for the future.

5. Conclusions

A relatively simple model of the processes responsible for the formation of cloud droplet spectra in nonprecipitating convective clouds was formulated for use in a multidimensional dynamical framework. The approach is based on four assumptions discussed in section 2b: 1) the amount of water substance subject to phase change is taken as predicted by the bulk microphysical model; 2) nucleation of cloud droplets is assumed to always produce the same initial droplet spectrum f_0; 3) further evolution of the cloud droplet spectrum is represented using base functions (elementary droplet populations) that are spectra generated from f_0 through further condensational growth; and 4) locally, droplet concentration corresponding to that at nucleation may only be present and any dilution of droplet concentration observed over model grid is always interpreted as a result of cloudy and cloud-free volumes coexisting inside the grid box.

The microphysical model was used with the cloud model of Clark (1977, 1979) to study the evolution of cloud droplet spectra in shallow (about 1.5 km deep) cumulus cloud. The cloud was growing in a conditionally unstable atmosphere capped by strong inversion at about 2 km. The cloud was forced by a prescribed low-level convergence zone. From the dynamical point of view, cloud was characterized by an adiabatic main updraft in the lower levels and complex bubblelike structures in the upper part resulting from the interactions between cloud and the overlaying inversion. Several interesting features were observed in the spectral evolution of cloud droplets. Within the lower part of the main updraft, monomodal distributions corresponding to the adiabatic spectrum were observed. Vortex-like structures in the upper part of the cloud were responsible for entrainment of environmental air, both from the side and from above the cloud top, leading to multimodal cloud droplet spectra as a result of fresh nucleation. In older parcels, complex (both broad and narrow, monomodal and multimodal) cloud droplet distributions were observed together with substantial cloud dilution.

This simulation produces interesting suggestions for further experimental studies. In particular, questions about the fine structure of the mixing regions as well as decaying parts of the convective cloud and droplet spectra were raised. Also, it has been suggested that in active cells with vortex-like structures located close to main updraft, spectra should be bimodal, with one peak corresponding to cloud base (adiabatic b value) and the second peak corresponding to a single entrainment level located at the base of the entraining vortex. This seems to be, at least to some degree, in line with observations of cumulus microphysics (e.g., Warner 1969a). An experiment with a new probe measuring droplet spatial distributions is planned to answer some of these questions and to gain better understanding of the mixing process inside cumulus clouds.

Acknowledgments. J.L.B. acknowledges the support of METEO-FRANCE, NATO, INSU (Grant 893613), and the Department of Atmospheric Sciences of the University of Wyoming. W.W.G. acknowledges the support of the Mesoscale and Microscale Meteorology Division of NCAR. Comments on the manuscript by Brad Baker, Terry Clark, and Paul Lawson are acknowledged. A thorough review and several critical comments by an anonymous reviewer were very helpful and led to the final version of this paper. The editorial support of Hope Hamilton is also acknowledged.

REFERENCES

Arakawa, A., 1966: Computational design for long-term numerical integration of the equations of fluid motions: Two-dimensional incompressible flow. *J. Comput. Phys.*, **1,** 119–143.

Austin, P. H., M. B. Baker, A. M. Blyth, and J. B. Jensen, 1985: Small scale variability in warm continental cumulus clouds. *J. Atmos. Sci.*, **42,** 1123–1138.

Baker, B. A., 1991: Turbulent entrainment and mixing in clouds, a new observational approach. *J. Atmos. Sci.*, **49,** 387–404.

Baker, M. B., R. G. Corbin, and J. Latham, 1980: The influence of entrainment on the evolution of cloud droplet spectra I: A model of inhomogeneous mixing. *Quart. J. Roy. Meteor. Soc.*, **106,** 581–598.

Bower, K. N., and T. W. Choularton, 1988: The effects of entrainment on the growth of droplets in continental cumulus clouds. *Quart. J. Roy. Meteor. Soc.*, **114,** 1411–1434.

Brenguier, J.-L., 1990: Parameterization of the condensation process in small nonprecipitating cumuli. *J. Atmos. Sci.*, **47,** 1127–1148.

——, 1991: Parameterization of the condensation process: A theoretical approach. *J. Atmos. Sci.*, **48,** 264–282.

Clark, T. L., 1977: A small-scale dynamic model using a terrain following coordinate transformation. *J. Comput. Phys.*, **24,** 186–215.

——, 1979: Numerical simulations with a three-dimensional cloud model: Lateral boundary condition experiments and multicellular severe storm simulations. *J. Atmos. Sci.*, **36,** 2191–2215.

——, and R. D. Farley, 1984: Severe downslope windstorm calculations in two and three spatial dimensions using anelastic interactive grid nesting: A possible mechanism for gustiness. *J. Atmos. Sci.*, **41,** 329–350.

Cooper, W. A., 1989: Effects of variable droplet growth histories on droplet size distributions. Part I: Theory. *J. Atmos. Sci.*, **46,** 1301–1311.

Grabowski, W. W., 1989: Numerical experiments on the dynamics of the cloud-environment interface: Small cumulus in a shear-free environment. *J. Atmos. Sci.*, **46,** 3513–3541.

——, and P. K. Smolarkiewicz, 1990: Monotone finite difference approximations to the advection–condensation problem. *Mon. Wea. Rev.*, **118,** 2082–2097.

Jensen, J. B., and M. B. Baker, 1989: A simple model for droplet spectral evolution during turbulent mixing. *J. Atmos. Sci.*, **46,** 2812–2829.

Lilly, D. K., 1962: On the numerical simulation of buoyant convection. *Tellus*, **14,** 148–172.

——, 1965: On the computational stability of numerical solutions of time-dependent nonlinear geophysical fluid dynamics problems. *Mon. Wea. Rev.*, **93,** 11–26.

Margolin, L. G., and P. K. Smolarkiewicz, 1989: Antidiffusive velocities for multipass donor cell advection. Lawrence Livermore National Laboratory. Report UCID 21866, 44 pp. [Available from National Technical Information Service, U.S. Department of Commerce, 5285 Port Royal Rd., Springfield, VA 22161.]

Mason, B. J., and C. W. Chien, 1962: Cloud droplet growth by condensation in cumulus. *Quart. J. Roy. Meteor. Soc.*, **88,** 136–142.

——, and P. R. Jonas, 1974: The evolution of droplet spectra and large droplets by condensation in cumulus clouds. *Quart. J. Roy. Meteor. Soc.*, **100,** 23–38.

Paluch, I. R., and C. K. Knight, 1984: Mixing and the evolution of cloud droplet size spectra in a vigorous continental cumulus. *J. Atmos. Sci.*, **41,** 1801–1815.

——, and D. G. Baumgardner, 1989: Entrainment and fine scale mixing in continental convective clouds. *J. Atmos. Sci.*, **46,** 261–278.

Pruppacher, H. R., and J. D. Klett, 1978: *Microphysics of Clouds and Precipitation,* D. Reidel, 422.

Raga, G. B., J. B. Jensen, and M. B. Baker, 1990: Characteristics of cumulus band clouds off the coast of Hawaii. *J. Atmos. Sci.*, **47,** 338–355.

Smagorinsky, J., 1963: General circulation experiments with the primitive equations. I. The basic experiment. *Mon. Wea. Rev.*, **91,** 99–164.

Smolarkiewicz, P. K., 1984: A fully multidimensional positive definite advection transport algorithm with small implicit diffusion. *J. Comput. Phys.*, **54,** 325–362.

——, and T. L. Clark, 1986: The multidimensional positive definite advection transport algorithm: Further development and applications. *J. Comput. Phys.*, **67,** 396–438.

——, and W. W. Grabowski, 1990: The multidimensional positive definite advection transport algorithm: Nonoscillatory option. *J. Comput. Phys.*, **86,** 355–375.

Sommeria, G., and J. W. Deardorff, 1977: Subgrid-scale condensation in model of nonprecipitating clouds. *J. Atmos. Sci.*, **34,** 344–355.

Srivastava, R. C., 1989: Growth of cloud droplets by condensation: A criticism of currently accepted theory and a new approach. *J. Atmos. Sci.*, **46,** 869–887.

Stith, J. L., and M. K. Politovich, 1989: Observations of the effects of entrainment and mixing on the droplet spectra in a small cumulus. *J. Atmos. Sci.*, **46,** 908–919.

Warner, J., 1969a: The microstructure of cumulus cloud. Part I. General features of the droplet spectrum. *J. Atmos. Sci.*, **26,** 1049–1059.

——, 1969b: The microstructure of cumulus cloud. Part II. The effect on droplet size distribution of the cloud nucleus spectrum and updraft velocity. *J. Atmos. Sci.*, **26,** 1272–1282.

——, 1973: The microstructure of cumulus cloud. Part IV. The effect on the droplet spectrum of mixing between cloud and environment. *J. Atmos. Sci.*, **30,** 256–261.